

A field study of free convection in an inclined-roof solar chimney

Sudaporn Chungloo^a, Bundit Limmeechokchai^{b,*}

^a Faculty of Architecture and Planning, Thammasat University, 99 Paholyothin Road, Pathumthani 12120, Thailand

^b Sirindhorn International Institute of Technology, Thammasat University, 99 Paholyothin Road, Pathumthani 12120, Thailand

*Corresponding author, e-mail: bundit@siit.tu.ac.th

Received 3 Apr 2008

Accepted 28 Apr 2009

ABSTRACT: A solar chimney is a hot air channel attached to the roof. It enhances natural ventilation for buildings by employing the temperature difference of air at the inlet and the outlet of the channel. Experiments were carried out in an open-ended air gap, situated between the corrugated roof tile and the gypsum board, with the tilt angle of 45° of the testing building. The results showed a reduction of temperature differences between the inlet and outlet of the solar chimney for all of the daytime, implying a decrease of volume flow rate of air in the system. The hot-surface, inlet air, and outlet air temperatures were observed to increase during 8:00–12:00 and they decreased rapidly during 13:00–17:00. We obtained an empirical equation relating the Nusselt number, Rayleigh number, and the dimensions and angles of the roof. Because the equation is derived from the field experiment under the hot and humid climate, it could be used for the determination of the mean convection heat transfer coefficient of a roof solar chimney with a similar geometry.

KEYWORDS: natural ventilation, low energy building, data relations, hot and humid climate

INTRODUCTION

The total heat transfer from a hot surface to the flowing air in a channel not only provides a temperature difference between the inlet air and the outlet air of the channel but also controls the amount of airflow through the channel. Therefore, the determination of the heat transfer coefficient (h) in the channel and the related Nusselt number (Nu) are essential in the simulation and application of passive ventilation. Empirical relations between the Nusselt number (Nu) and the Rayleigh number (Ra) have been derived for a wide range of Ra values, heated plate-air temperature differences and various tilt angles. A relationship between Nu and Ra have been proposed by Ostrach¹ as $Nu = (Ra Pr)^{0.25}$ using the scaling analysis of the fluid with Prandtl number (Pr), $Pr \ll 1$. Azevedo and Sparrow² found the relation $Nu_s = 0.645[Ra_s(S/L)]^{0.25}$ for the symmetric isothermal plates and isothermal-insulated plates by carrying out experiments on the inclined channels in water. Hirunlabh et al³ showed that Nu and air flow rate in the application of the inclined solar chimney can be computed by using the relation derived for an inclined enclosure^{4,5}. For various values of uniform heat flux applied to a rectangular channel heated from the top, Bunnag et al⁶ obtained $Nu =$

$139.25(Ra \sin \theta)^{1.238}(S/L)^{6.896}$ for the channel tilt angles (θ) of 15–75°. Despite the derivation of general relationships of Nu of various channel configurations, a specific relationship with particular temperature difference is necessary to determine the exact value of Nu . The analysis of the data on the experiment in the laboratory⁷ showed that an inclined channel of parallel plates with temperature varying from 40–70 °C gives $Nu_s = 1.227[(S/L)Ra_s \sin 30^\circ]^{0.2916}$. The derived heat transfer coefficients are between 6.76 and 10.26 W/m²K⁷.

In addition to the need of an exact relation for Nu for a particular application, the free convection in the open ended channel, such as the application of a solar chimney in the outdoor field, have been required. Practically, the induced ventilation alters all of the day hours because of the heat loss from the solar collected surface, i.e. roof tile of the solar chimney, the wind effects, the ambient temperature and the sky radiation. By using the experimental data collected from the installed solar chimney, this paper obtains a relation between Nu , the Reynolds number (Re), Ra_s , and the air gap/length ratio. The capability to induce ventilation of the existing solar chimney system is also studied.

We investigated the temperature differences $T_h -$

T_b and $T_o - T_i$, where T_h , T_i , and T_o , are the hot surface, inlet and outlet air temperatures. They were explained in the contexts of solar radiation and ambient air temperature concurrently because the solar chimney was enclosed by a cover at the outlet and connected to the room at the inlet. The inlet and outlet are separate from the ambient areas. Unlike the open-ended channel where both ends are exposed to the ambient areas, $T_h - T_b$ and $T_o - T_i$ show a closer relationship with the heat transfer rate (Q) and volume flow rate (VFR) than those with the ambient temperature. In addition, the variation of wind velocity produces uncertainty in the relation with those temperature differences and the wind effect is excluded in this study. To enhance the buoyancy force and to increase the airflow rate, the tilt angle of the applied solar chimney was increased from a typical values of $20\text{--}30^\circ$ to the tilt angle of 45° ^{6,8}. The relationships between $T_h - T_b$, $T_o - T_i$, T_h , T_o and T_i and the solar radiation in the morning hours and in the afternoon hours were proposed by taking into account that the ambient temperature in the morning is lower than in the afternoon. Due to the complication of the effect of the ambient conditions on the volume flow rate, the relations governing a solar chimney are related to the heat source i.e., the value of $T_h - T_b$. Therefore, the values of temperature difference, $T_o - T_i$, heat transferred to the air, Q/A , and volume flow rate (VFR) are linearly related with $T_h - T_b$ and were used to derive equations to predict the relationships of Nu_s and Re_s .

EXPERIMENTAL SETUP AND METHODS

The experiments were carried out in one of the four channels of the solar chimney installed above the room of a testing building. For the testing building, the corrugated roof tiles are fixed over the 45° inclined wooden structure of the roof which face the south direction and is heated up by the sun during the daytime. A gypsum board covers the lower part of inclined wooden structure and the external surface faces the air in the attic above the ceiling (Fig. 1). The walls of the room are composed of polystyrene foam 70 mm thick as the insulation inserted between two wooden boards 9 mm thick. Connected to the mobile data logger, two hot-bulb probes are used to measure air velocity at the inlet and at the outlet of the channel which are opened to the room air and outdoor, respectively. Recorded by a pyranometer Kipp&Zonen-CM11 and Yong wind monitor, the outdoor conditions such as solar intensity and wind velocity are connected to a Yokogawa data logger to record the data simultaneously every 2 mins during the daytime in summer and average it every 10

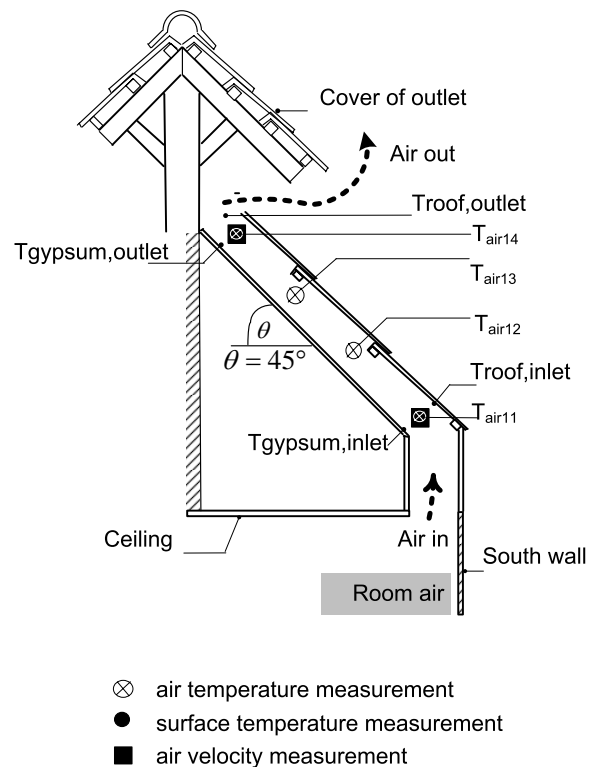


Fig. 1 Schematic representation of experimental set-up of the solar chimney.

mins.

The positions of temperature and velocity measurement are shown in Fig. 2. The total width (W), length (L) and aspect ratio (S/L) of the solar chimney are 960 mm, 1660 mm and 0.115 respectively. The channel space (S) of 185 mm is the maximum distance between the gypsum surface and the surface of the corrugated roof. There are 16 type-k thermocouples used to measure temperature, 8 for measuring air temperature of the channel, 4 for measuring surface temperature of roof tiles and gypsum boards, 3 for measuring air in the room, and 1 for measuring temperature of the outdoor air. All thermocouples are connected to the Yokogawa-DR130 data logger and the experiments were carried out on 5 selected days in May and June.

EXPERIMENTAL RESULTS

The effect of solar radiation

Since the volume flow rate of air depends on the differences values of $T_h - T_b$ and the $T_o - T_i$, the investigation of these values displays the capability of the application of a solar chimney. The effect of solar radiation on the air temperature differences

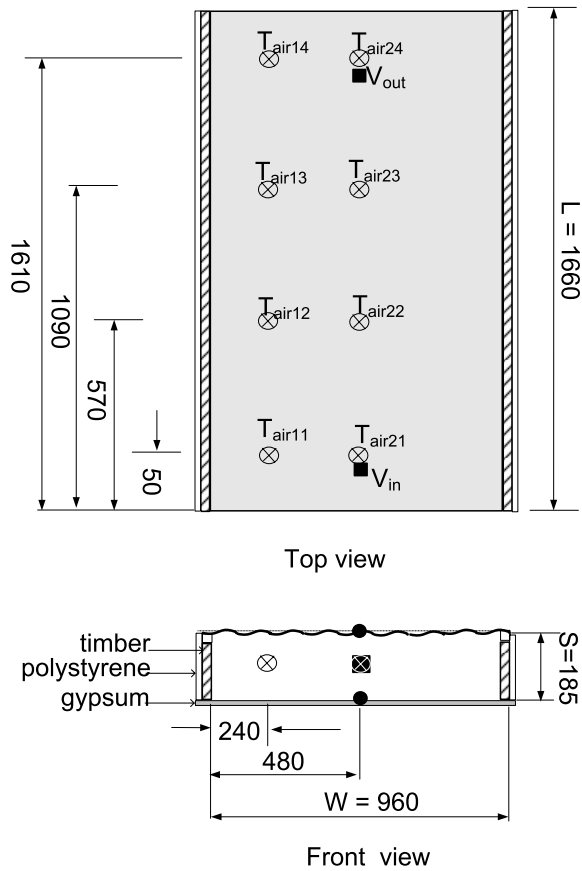


Fig. 2 Positions of measuring temperature and velocity of air. All dimensions are in mm.

is shown in Fig. 3a by plotting the mean values of $T_h - T_b$ and the $T_o - T_i$ against the solar radiation. With the low values of correlation coefficient, R^2 , the linear relationship between these temperature differences and solar radiation are shown. According to the experimental results in Fig. 3a, the effect of solar radiation on $T_o - T_i$ and $T_h - T_b$ can be divided into three sections: (1) reverse flow, $G < 200 \text{ W/m}^2$, $T_o - T_i \leq 0^\circ\text{C}$ and $0 < T_h - T_b \leq 2$, (2) oscillation, $200 < G \leq 500 \text{ W/m}^2$, $0^\circ\text{C} < T_o - T_i \leq 5^\circ\text{C}$ and $3^\circ\text{C} < T_h - T_b \leq 7^\circ\text{C}$, and (3) escalation, $500 < G < 1000 \text{ W/m}^2$, $0^\circ\text{C} < T_o - T_i \leq 6^\circ\text{C}$ and $3^\circ\text{C} < T_h - T_b \leq 8^\circ\text{C}$.

Theoretically, the solar induced ventilation starts when the temperature differences $T_o - T_i$ are greater than 0°C . Since the room is insulated and the solar radiation is too low to produce air flow out of the building and the air temperature at the outlet (T_o) is lower than that of the inlet (T_i) and of the room, the reverse flow i.e. airflow from the channel to the room, occurs in the early morning and late evening. This

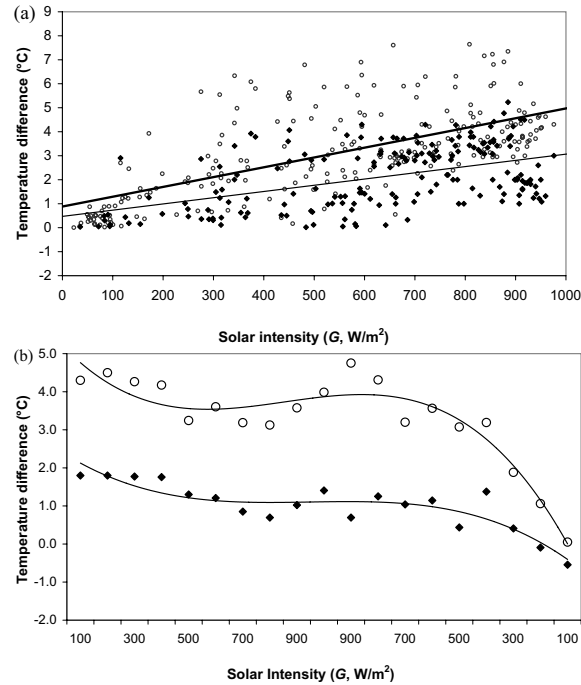


Fig. 3 Experimental results of temperature differences, $T_h - T_b$ (diamonds) and $T_o - T_i$ (circles), vs. solar intensity. (a) Experimental results and linear relationships: $T_h - T_b = 0.004G + 0.883$, $R^2 = 0.43$ and $T_o - T_i = 0.003G + 0.473$, $R^2 = 0.24$. (b) Mean values.

shows that the solar chimney can be used for enhancing cool air induced into the room during the early morning and evening. For values of solar radiation greater than 200 W/m^2 but less than 500 W/m^2 , the values of $T_o - T_i$ and $T_h - T_b$ vary all the time since the cloud obstructs the solar radiation frequently and the surface and air temperatures changes slowly due to thermal inertia. For instance, the experimental data show that the values of $T_h - T_b$ oscillate between 1 and 6°C for the change of solar radiation around 400 W/m^2 . At values of solar intensity greater than 500 W/m^2 , the values of $T_o - T_i$ and $T_h - T_b$ increase consistently. The maximum values of $T_h - T_b$ and $T_o - T_i$ are 8 and 5°C , respectively, for the solar intensity of 950 W/m^2 .

The effect of ambient air

The study of the experimental data shows that the effect of ambient temperatures on the temperature differences, $T_h - T_b$ and $T_o - T_i$, in the morning are different from those in the afternoon. Given that the ambient temperature in the morning is lower than that in the afternoon, the process of heat transfer from the heated roof to the air is faster than that in the

afternoon. The experimental data of $T_h - T_b$ and $T_o - T_i$ are categorized along with the values of solar radiation, ranging from 0–100, 100–200, 200–300, 400–500, ..., 900–1000 W/m^2 , and the time periods in morning and afternoon (Fig. 3b). The mean values of $T_h - T_b$ are derived with the standard deviation of 0.41–1.92 and 0.25–2.04 for the morning hours and afternoon hours, respectively. The mean values of $T_o - T_i$ are derived with the standard deviation of 0.19–1.56 and 0.57–1.62 for the morning hours and afternoon hours, respectively. The high deviation values of $T_h - T_b$ and $T_o - T_i$ indicate the rapid change of solar radiation due to the cloud. The regression analysis of the mean values and the solar radiation clearly show that the values of $T_h - T_b$ and $T_o - T_i$ decrease as the solar radiation increase in the morning but they decrease with the solar radiation decrease in the afternoon. The larger decrease of temperature differences in the afternoon than those in the morning implies that the utilization of a solar chimney in the afternoon provides less ventilation than that in the morning.

The investigation of relationships of T_h , T_o , and T_i along with the solar radiation are shown as the linear relationships in Fig. 4a for the morning time: $T_h = 0.0054G + 31.35$; $R^2 = 0.93$, $T_o = 0.0061G + 27.78$; $R^2 = 0.97$, $T_i = 0.0077G + 25.72$; $R^2 = 0.97$. The quadratic relationships in Fig. 4b are suggested for the afternoon time as $T_h = (-2G^2/10^5) + 0.024G + 30.87$, $R^2 = 0.95$, $T_o = (-G^2/10^5) + 0.016G + 30.73$, $R^2 = 0.97$, $T_i = (-G^2/10^5) + 0.013G + 30.96$, $R^2 = 0.81$.

As a result of the high deviation of surface and air temperatures collected for solar radiation between 200–500 W/m^2 , the derived relationships here include the effect of shading from clouds.

THE DATA ANALYSIS

Nu_s is evaluated by

$$Nu_s = (hS)/k, \tag{1}$$

where k is the thermal conductivity of air and

$$h = Q/[A_{eff}(T_h - T_b)], \tag{2}$$

where $A_{eff} = WL$ is the effective area.

As the heat loss from the roof tiles and gypsum board and radiative exchange are neglected, Q , the heat transfer rate of the roof tile, can be computed from

$$Q = m'c_p(T_o - T_i), \tag{3}$$

where $m' = \rho A_{channel}V$ is the mass flow rate of air where ρ is the density of air, $A_{channel} = SW$ is the

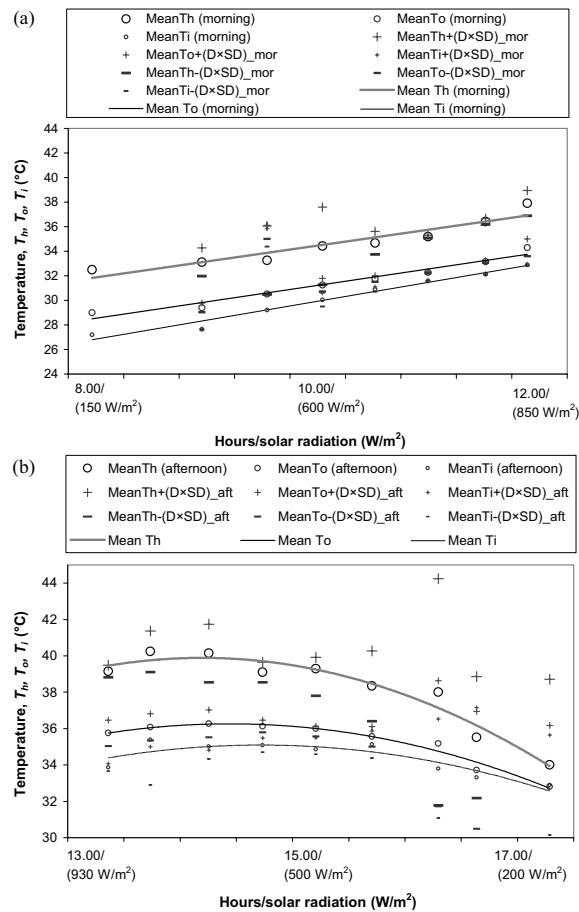


Fig. 4 Experimental results of surface temperature (T_h), inlet (T_o), and outlet (T_i) air temperature of the solar chimney plotted against solar intensity (W/m^2). (a) the morning hours (b) the afternoon hours. D is 95% confidence interval. SD = standard deviation.

effective area of the channel, V is the velocity of air and c_p is the specific heat of air. The Nu_s results will be related with Ra_s which is given by

$$Ra_s = [g\beta(T_h - T_b)S^3/\nu^2]Pr, \tag{4}$$

where g is the gravitational acceleration, β is the coefficient of thermal expansion of air, and ν is the kinematic viscosity of air.

All thermophysical properties of air are evaluated at the bulk temperature of air, T_b . By using the trapezoidal rule⁷, T_b in this study can be estimated from

$$T_{b1} = \frac{1}{8}(T_{air11} + 3T_{air12} + 3T_{air13} + T_{air14}), \tag{5}$$

$$T_{b2} = \frac{1}{8}(T_{air21} + 3T_{air22} + 3T_{air23} + T_{air24}), \tag{6}$$

$$T_b = (T_{b1} + T_{b2})/2. \tag{7}$$

The temperature of the air at the inlet T_i is computed from average values of temperature of room air near the ceiling. The air temperature at the outlet T_o and the temperature of internal surface of roof tile, T_h are from experimental results.

The VFR of air in the solar chimney can be estimated by

$$\text{VFR} = C_D A_{\text{channel}} [g L \sin 45^\circ (T_o - T_i) / T_i]^{1/2}, \quad (8)$$

where the value of C_D , coefficient of discharge, in this study is 0.4⁹. The Reynolds number is calculated from

$$\text{Re}_s = (VS/\nu). \quad (9)$$

Data analysis

The purpose of the data analysis is to obtain linear relationships between $T_h - T_b$ and other variables such as heat transfer rate per area Q/A , temperature difference at the inlet and outlet, $T_o - T_i$ and VFR before determination of values of Nu_s , Re_s , and Ra_s .

The linear relationships between $T_h - T_b$ and $T_o - T_i$, Q/A and VFR are shown in Fig. 5a, 5b, and 5c, respectively. The calculated values of $T_o - T_i$, Q/A and VFR using the derived linear equations and the calculated values of velocity (V) and convective coefficient, (h) using (2) and (8) are summarized in Table 1. It is shown in Table 1 that the value of $T_h - T_b = 0^\circ\text{C}$ provides the negative value of $T_o - T_i$. The values of $T_h - T_b$ in the range of 1.37–2.00 $^\circ\text{C}$ give the positive value of $T_o - T_i$ of 0.01–0.39 $^\circ\text{C}$ and the value of $T_h - T_b = 3^\circ\text{C}$ creates the air temperature difference $T_o - T_i$ of 1 $^\circ\text{C}$. Hence, the values of Nu_s , Re_s and Ra_s shown in Table 1 are computed for the range of temperature difference $3^\circ\text{C} \leq T - T_b \leq 9^\circ\text{C}$ to display the airflow ventilation from the room to the solar chimney.

Nu_s is the non-dimensional expression of heat transfer coefficient, h , as $\text{Nu}_s = hS/k$. The relations between Nusselt number and Rayleigh number, angle of channel and aspect ratio (S/L) are typically in the form

$$\text{Nu}_s = a[(S/L)\text{Ra}_s \sin \theta]^b. \quad (10)$$

Based on the value of Ra_s and Nu_s in Table 1, the constants a and b are obtained by means of least square analysis of the logarithms of (10) as follows:

$$\text{Nu}_s = 1.444[(S/L)\text{Ra}_s \sin 45^\circ]^{0.249}. \quad (11)$$

The Reynolds number, Re_s , is the non-dimensional expression of velocity, V . The expression of Reynolds number as the function

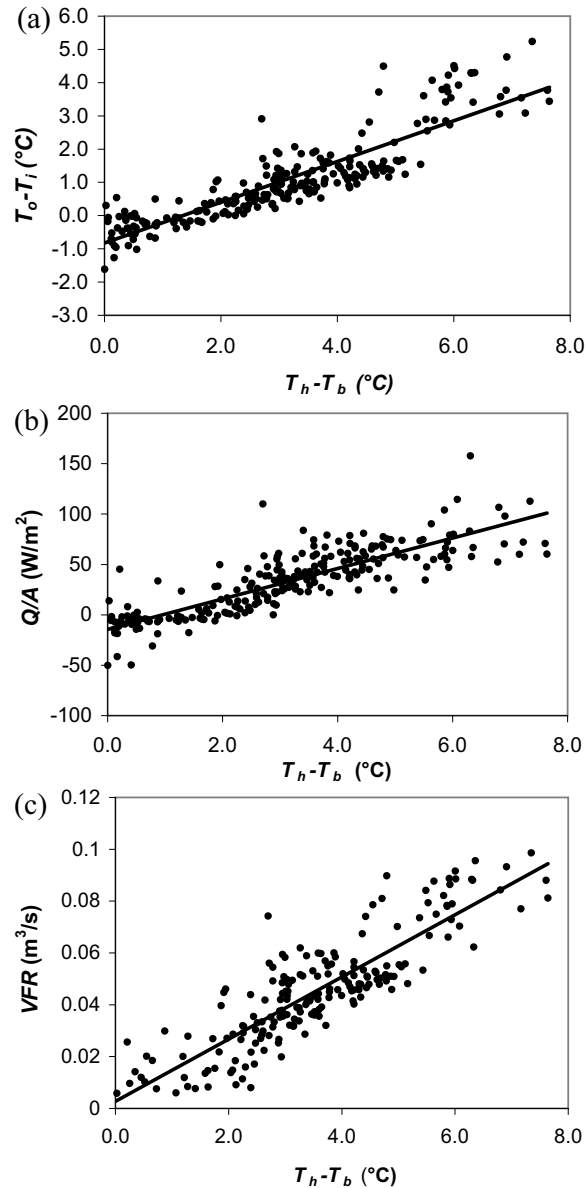


Fig. 5 Linear relationships between $T_h - T_b$ and $T_o - T_i$, Q/A , and VFR. (a) $T_o - T_i = 0.61(T_h - T_b) - 0.83$, $R^2 = 0.81$, $SD = 2.09$. (b) $Q/A = 15.10(T_h - T_b) - 14.39$, $R^2 = 0.75$, $SD = 0.18$. (c) $\text{VFR} = 0.012(T_h - T_b) - 0.003$, $R^2 = 0.75$, $SD = 0.014$.

of Rayleigh number, angle of channel, and aspect ratio (S/L) are in the following forms⁷:

$$\text{Re}_s = (VS)/\nu = \exp[a + b(S/L)\text{Ra}_s \sin 45^\circ], \quad (12)$$

$$\text{Re}_s = \exp[6.884 + 5.538 \times 10^{-7}(S/L)\text{Ra}_s \sin 45^\circ] \quad (13)$$

For (11) and (13), the range of Ra_s is

Table 1 Summary of the experimental and calculated data.

Quantity	$S/L = 0.1145$									
<i>Variables related to $T_h - T_b$</i>										
$T_h - T_b$ (°C)	0	1.37	2	3	4	5	6	7	8	9
$T_o - T_i$ (°C)	-0.83	0.01	0.39	1.00	1.61	2.22	2.83	3.44	4.05	4.66
Heat transfer rate (Q/A) (W/m ²)	-14.387	6.30	15.82	30.92	46.02	61.12	76.23	91.33	106.43	121.53
Air volume flow rate (VFR) (m ³ /s)	-	0.02	96.12	139.32	182.52	225.72	268.92	312.12	355.32	398.52
<i>Calculated variables</i>										
Average velocity (m/s)	0.02	0.10	0.15	0.21	0.28	0.34	0.41	0.47	0.54	0.60
Convective coefficient (W/m ² K)	-	2.86	4.91	6.40	7.15	7.59	7.89	8.10	8.26	8.39
<i>Non-dimensional parameters</i>										
Nusselt number	-	20.46	35.14	45.75	51.02	54.15	56.21	57.66	58.74	59.56
Reynolds number ($\times 10^3$)	0.000	0.345	1.058	1.767	2.473	3.175	3.874	4.570	5.262	5.950
Prandtl number	0.71	0.71	0.71	0.71	0.71	0.71	0.71	0.71	0.71	0.71
Rayleigh number ($\times 10^6$)	-	7.25	10.47	15.44	20.24	24.87	29.36	33.69	37.88	41.93
$(S/L)Ra_s \sin 45^\circ$ ($\times 10^6$)	-	0.588	0.847	1.249	1.638	2.013	2.376	2.727	3.066	3.394

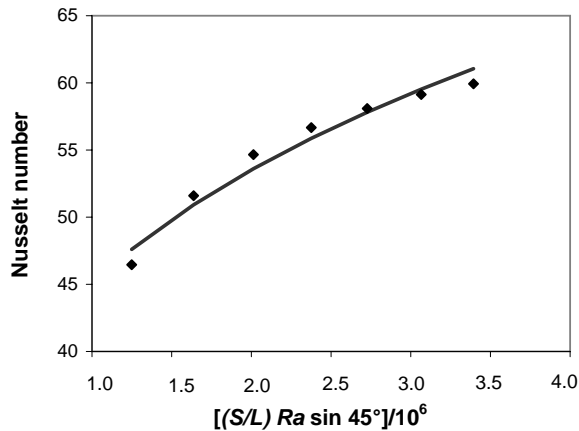


Fig. 6 Nusselt number vs. $(S/L)Ra_s \sin 45^\circ$.

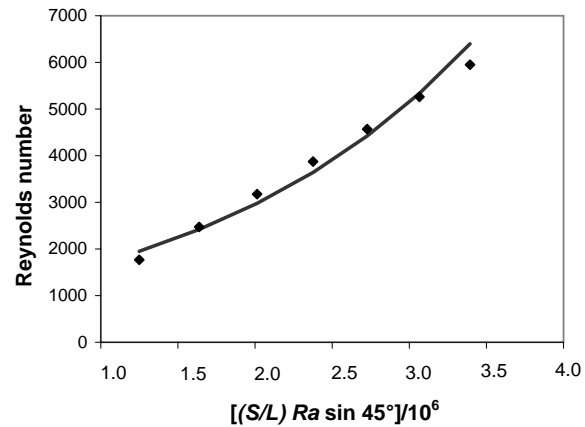


Fig. 7 Reynolds number vs. $(S/L)Ra_s \sin 45^\circ$.

$1.543 \times 10^7 < Ra_s < 4.193 \times 10^7$ and the range of $T_h - T_b$ is $3.00^\circ\text{C} \leq T_h - T_b \leq 9.00^\circ\text{C}$. The computational results of (11) and (13) are shown as solid lines in Fig. 6 and Fig. 7, respectively.

DISCUSSION

Under the conditions of a hot and humid climate, free convection was studied in a hot air channel of a 45° inclined roof solar chimney. The investigation included collecting data of surface and air temperatures in the channel, analysing experimental data and determining the relation between the three non-dimensional quantities Nu_s , Ra_s , and Re_s , the aspect ratio (gap/length), and the angle of inclination. The effect of solar radiation and the ambient temperature on the temperature differences $T_h - T_b$ and $T_o - T_i$ were investigated. It was concluded that both of the

temperature differences reduce all the day and the temperature differences in the afternoon reduce faster than those in the morning. Hence, the volume flow rate of air decreases all day since the volume flow rate of the buoyancy driven system depends on the temperature differences. Therefore, the application of a solar chimney in the hot and humid climate needs pre-cooled inlet air⁹ or a modification of the bioclimatic roof¹⁰ to improve the temperature differences especially during the afternoon hours.

The observation of our solar chimney showed that the values of temperature differences, T_h , T_o , and T_i , were functions of the solar radiation and the ambient temperature. Although the solar radiation is the heat source of the solar chimney, the data analysis of $T_o - T_i$, Q/A , and VFR was carried out as linear function against $T_h - T_b$ because the $T_h - T_b$ also

varies with ambient conditions. For the values of T_h , T_o , and T_i , the linear relationships with the solar radiation were suggested for the morning hours and the quadratic relationships for the afternoon hours. Due to the complicated interaction with ambient conditions, capability to induce air flow rate in a solar chimney are found to be more precisely related to the heat source of the solar chimney than to the ambient conditions. In addition, the effects of rapid change of solar radiation on the surface temperature, air temperature and temperature differences, $T_h - T_b$ and $T_o - T_i$, are included in the derived relationships.

With the typical values of $3.0^\circ\text{C} \leq T_h - T_b \leq 8.0^\circ\text{C}$ and similar geometry of a solar chimney, this study proposes two empirical relations for determination of convective heat transfer coefficient and air flow rate developed in the solar chimney, the relation between Nu_s and Ra_s and relation between Re_s and Ra_s , respectively. The derived relation between Nu_s and Ra_s is $Nu_s = 1.444[(S/L)Ra_s \sin 45^\circ]^{0.249}$. The power of 0.249 is close to the traditional value of 0.25 found by Ostrach¹. Compared with the laboratory results and the relation found by Khedari et al⁷, the solar chimney in this study deals with a larger aspect ratio, higher angle of inclination, higher value of Ra_s and smaller range of values of $T_h - T_b$ (Table 1). The derived relation between Re_s and Ra_s computed from (12) is $Re_s = \exp[6.884 + (5.538/10^7)(S/L)Ra_s \sin 45^\circ]$.

In addition to the relations for a solar chimney used in the field, this study verifies the results of previous studies that indicate that a solar chimney with high tilt angle increases the capability to induce ventilation^{6,8}. By using the relation between the non-dimensional quantities for $3.0^\circ\text{C} \leq T_h - T_b \leq 8.0^\circ\text{C}$, this study found the values of convective heat transfer coefficient of 4.91–8.39 W/m²K and the calculated values of air flow rate of 9.72–398.52 m³/hour. Comparing to the value of heat transfer coefficient of 6.76–10.26 W/m²K and ventilating airflow of 181.12–319.62 m³/hour found in Ref. 7 for $8.71^\circ\text{C} \leq T_h - T_b \leq 37.42^\circ\text{C}$, this study shows higher values of heat transfer coefficient for a smaller range of $T_h - T_b$. According to Bunnag et al⁶, the results of high ventilating airflow in this study is related to the high value of heat transfer coefficient and the decrease of temperature difference $T_h - T_b$.

REFERENCES

- Ostrach S (1953) An analysis of laminar free convection flow and heat transfer about a flat plate parallel to the direction of the generating body force. Report 1111, National Advisory Committee for Aeronautics.
- Azevedo LFA, Sparrow EM (1985) Natural convection in open-ended inclined channels. *J Heat Tran* **107**, 893–901.
- Hirunlabh J, Wachirapuwadon S, Pratinthong N, Khedari J (2001) New configurations of a roof solar collector maximizing natural ventilation. *Build Environ* **36**, 383–91.
- Hollands KGT, Unny SE, Raithby GD, Konicek L (1976) Free Convective Heat Transfer Across inclined air layers. *J Heat Tran* **98**, 189–93.
- Gebhart B (1971) *Heat Transfer*, 2nd edn, New York, McGraw-Hill.
- Bunnag T, Khedari J, Hirunlabh J, Zeghmati B (2004) Experimental investigation of free convection in an open-ended inclined rectangular channel heated from the top. *Int J Ambient Energ* **25**, 151–62.
- Khedari J, Yimsamerjit P, Hirunlabh J (2002) Experimental investigation of free convection in roof solar collector. *Build Environ* **37**, 455–9.
- Susanti L, Homma H, Matsumoto H, Suzuki Y, Simizu M (2008) A laboratory experiment on natural ventilation through a roof cavity for reduction of solar heat gain. *Energ Build* **40**, 2196–206.
- Chungloo S, Limmeechokchai B (2007) Application of passive cooling systems in the hot and humid climate: The case study of solar chimney and wetted roof in Thailand. *Build Environ* **42**, 3341–51.
- Waewsak J, Hirunlabh J, Khedari J, Shin UC (2003) Performance evaluation of the BSRC multi-purpose bio-climatic roof. *Build Environ* **38**, 1297–302.